



Published in final edited form as:

ACS Chem Biol. 2015 August 21; 10(8): 1778–1784. doi:10.1021/acscchembio.5b00213.

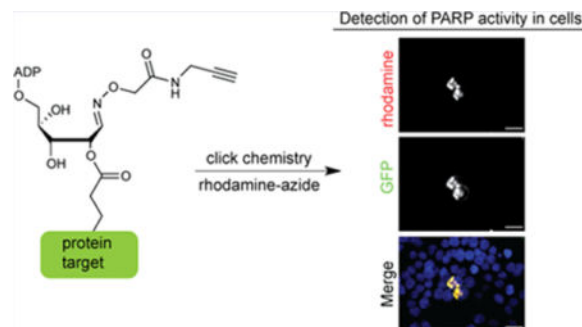
A Clickable Aminoxy Probe for Monitoring Cellular ADP-Ribosylation

Rory K. Morgan and Michael S. Cohen*

Program in Chemical Biology and Department of Physiology and Pharmacology, Oregon Health & Science University, Portland, Oregon 97210, United States

Abstract

ADP-ribosylation is essential for cell function, yet there is a dearth of methods for detecting this post-translational modification in cells. Here, we describe a clickable aminoxy alkyne (AO-alkyne) probe that can detect cellular ADP-ribosylation on acidic amino acids following Cu-catalyzed conjugation to an azide-containing reporter. Using AO-alkyne, we show that PARP10 and PARP11 are auto-ADP-ribosylated in cells. We also demonstrate that AO-alkyne can be used to monitor stimulus-induced ADP-ribosylation in cells. Functional studies using AO-alkyne support a previously unknown mechanism for ADP-ribosylation on acidic amino acids, wherein a glutamate or aspartate at the initial C1'-position of ADP-ribose transfers to the C2' position. This new mechanism for ADP-ribosylation has important implications for how glutamyl/aspartyl-ADP-ribose is recognized by proteins in cells.



ADP-ribosylation has emerged as a major post-translational modification in cells. ADP-ribosylation is catalyzed by a family of 17 enzymes in humans known as poly-ADP-ribose polymerases (PARPs), which transfer ADP-ribose (ADPr) from nicotinamide adenine dinucleotide (NAD^+) to amino acids on target proteins to form monomers (mono-ADP-ribosylation) or polymers (poly-ADP-ribosylation) of ADPr.¹ Despite their name, the majority of the PARP family members catalyze mono-ADP-ribosylation; in fact, only four

*Corresponding Author: Phone: 503.418.1363. cohenmic@ohsu.edu.

Supporting Information

Supporting Scheme 1 showing the synthesis of the AO-Alkyne probe, Supporting Figures 1–4, and compound characterization. The Supporting Information is available free of charge on the ACS Publications website at DOI: 10.1021/acscchembio.5b00213.

Notes

The authors declare no competing financial interest.

PARPs (PARP1, 2, 5a/b) have been shown to be *bona fide* poly-ADPr polymerases.² Methods for detecting ADP-ribosylation in general, and mono-ADP-ribosylation in particular, in cells are lacking. The use of radiolabeled NAD⁺ and NAD⁺ variants, such as biotin-NAD⁺³ or 6-alkyne-NAD⁺,^{4,5} followed by click chemistry with an azide reporter has been useful for detecting mono-ADP-ribosylation *in vitro* but cannot be used for detecting ADP-ribosylation in cells. We therefore sought a strategy for detecting ADP-ribosylation in cells.

We focused our initial efforts on detecting proteins modified by ADPr on the acidic amino acids glutamate (Glu) and aspartate (Asp) since recent proteomics studies demonstrate that these are major sites of ADP-ribosylation in the cell.^{6,7} Seminal studies in the late 1970s demonstrated that the Glu- and Asp-ADPr bond is cleaved rapidly by high concentrations of hydroxylamine.^{8,9} The proposed mechanism for this cleavage involves transacylation from the ester between Glu or Asp and ADPr to hydroxylamine, resulting in the formation of a hydroxamic acid derivative at the site of modification, with concomitant release of free ADPr. This mechanism was exploited in a recent study that sought to characterize the Glu/Asp-ADP-ribosylated proteome.⁷ Based on this mechanism, we designed an aminoxy alkyne probe (AO-alkyne, **1**) (Figure 1a and Supporting Scheme 1) for the detection of mono-ADP-ribosylation of proteins on acidic amino acids. We envisioned that AO-alkyne would react with the ester of Glu/Asp-ADPr forming an alkyne hydroxamic ester that could be subsequently detected after Cu-catalyzed conjugation (“click chemistry”) to an azide reporter.

We first determined if **1** could detect PARP10-mediated ADPr modification of SRSF protein kinase 2 (SRPK2; Figure 1b). Previous studies demonstrated that SRPK2 is a substrate of PARP10,^{10,11} which transfers ADPr onto acidic amino acids in target proteins.¹² We treated human PARP10 catalytic domain (hPARP10_{cat}) and SRPK2 with NAD⁺ (100 μM) and then added **1** (100 μM) at various pH values followed by click conjugation to a biotin-azide reporter. Labeling of SRPK2 by **1** was NAD⁺-dependent and maximal at pH 5 (Figure 1c). In contrast, no labeling was detected at pH values greater than 7 (Figure 1c). These observations are inconsistent with a mechanism involving transacylation of the ester modification linking ADPr to its protein target, which occurs at neutral and slightly basic pH values. Instead, we hypothesize that **1** forms an oxime bond with Glu/Asp-ADPr on SRPK2, the formation of which is optimal at pH 4–5. Recently, it was shown that substituted anilines catalyze oxime bond formation at neutral pH.¹³ Indeed, when *p*-phenylenediamine (PDA) was added together with **1** at pH 7, we observed labeling of Glu/Asp-ADP-ribosylated SRPK2 (Figure 1d). The less effective oxime catalyst, aniline, did not result in labeling (Figure 1d). Using our optimized labeling conditions, we were also able to detect ADP-ribosylation of SRPK2 by another PARP, PARP15, which catalyzes mono-ADP-ribosylation (Supporting Figure 1).² Taken together, these results suggest that **1** is reacting with an aldehyde that is present on Glu/Asp-ADPr, leading to formation of a stable oxime.

The terminal ribose ring of free ADPr tautomerizes between a ring-closed and a ring-opened form; the latter form contains an aldehyde at the C1'-position capable of reacting with an amino-oxy group at pH 4–5.¹⁴ If PARP10-mediated ADP-ribosylation of acidic amino acids involves the formation of a glycoside bond between Glu/Asp and the C1'-position of the

terminal ribose ring—which is the currently accepted model for ADP-ribosylation of acidic amino acids¹²—how does **1** react with Glu/Asp-ADPr to form an oxime? We propose that a transfer of the Glu/Asp from the C1' position to another site (i.e., C2') on the ribose ring is occurring (Figure 2a). This proposed C1'–C2' transfer frees up the C1' position, enabling **1** to react with the open-chain aldehyde form at C1' at acidic pH or in the presence of PDA catalysis at neutral pH.

To test this proposed mechanism, we treated Glu/Asp-ADP-ribosylated SRPK2 with sodium borohydride (NaBH₄), which should reduce the C1' aldehyde, preventing oxime bond formation with an aminoxy probe. Indeed, we found that increasing concentrations of NaBH₄ blocked labeling of Glu/Asp-ADP-ribosylated SRPK2 by aminoxy-biotin (AO-biotin; Figure 2b). While ester bonds are stable to NaBH₄ reduction,¹⁵ we wanted to rule out hydrolysis of ADPr at the ester linkage due to an increase in pH from NaBH₄ decomposition in aqueous medium. We repeated the previous borohydride reduction experiment using an NAD⁺ variant containing an alkyne modification at the N6 position of the adenosine ring (6-a-NAD⁺)^{4,5} instead of native NAD⁺. The alkyne handle can be conjugated to an azide reporter and provides a secondary means to detect ADPr modification. Whereas NaBH₄ blocked AO-biotin-mediated labeling of 6-a-ADP-ribosylated SRPK2, it did not block click-chemistry-mediated labeling of 6-a-ADP-ribosylated SRPK2 with biotin-azide (Figure 2c). Therefore, the Glu/Asp-ADPr modification does not undergo hydrolysis at the ester linkage under reaction conditions that contain NaBH₄, remaining attached to its protein target SRPK2. Together, these results support the presence of an aldehyde at the C1' position of Glu/Asp-ADPr that is capable of reacting with an aminoxy probe.

Our proposed mechanism suggests that a C1'-aldehyde and a C2'-Glu/Asp ester exist on the same ADPr modification site. To examine this idea, we determined if we could simultaneously label 6-a-Glu/Asp-ADP-ribosylated SRPK2 with an aminoxy TAMRA (AO-TAMRA) probe and an Alexa Fluor 488-azide (AF488-azide) probe using click chemistry. We found that 6-a-Glu/Asp-ADP-ribosylated SRPK2 is labeled with both fluorescent probes, as demonstrated by in-gel fluorescence scanning (Figure 2d). Taken together, our results support our proposed mechanism in which the Glu/Asp that is initially attached to the C1' position of ADPr is transferred to the C2' position, where transfer to the C3' position could also occur due to a C2'–C3' equilibrium.

Recently, two independent studies demonstrated that a family of macrodomain-containing proteins (MacroD1 and D2) reverses mono-ADP-ribosylation on acidic amino acids on proteins.^{16,17} The authors propose two divergent mechanisms of mono-ADPr reversal: in one study, the authors propose that the acidic amino acid is attached to the C1' position and that MacroD's hydrolyze the glycosidic bond between Glu/Asp and ADPr;¹⁶ in the other study, the authors propose that the acidic amino acid is attached to the C2' position and that MacroD's hydrolyze the ester bond between Glu/Asp and ADPr.¹⁷ The latter model is based on the structural similarity between ADPr and the sirtuin deacetylation product 2'-O-acetyl-ADPr, which was the first characterized substrate of MacroD's.^{18,19} Our results support the second model of MacroD-mediated reversal of ADP-ribosylation on acidic amino acids.

Having examined the mechanism of PARP10-mediated ADP-ribosylation of acidic amino acids, we next sought to determine if **1** could detect mono-ADP-ribosylation of PARP10 in cells. Human embryonic kidney (HEK) 293T cells expressing GFP-tagged PARP10 (GFP-PARP10 WT) were treated with **1** (100 μ M) in the presence of the oxime catalyst PDA. Click conjugation of biotin-azide in lysates derived from GFP-PARP10 WT transfected HEK 293T cells resulted in labeling of a single band \sim 175 kDa, which is the size of GFP-PARP10 WT (Figure 3a). No labeling was observed without the oxime catalysis or in the presence of aniline, consistent with our *in vitro* studies (Supporting Figure 2). To determine if this labeling is due to PARP10 catalytic activity, we performed the same experiment with a catalytically inactive PARP10 mutant, PARP10 G888W (GFP-PARP10 GW).²⁰ In contrast to results with GFP-PARP10 WT, no labeling was observed in GFP-PARP10 GW expressing cells (Figure 3a). These results are consistent with PARP10 undergoing automodification in cells, which has been demonstrated previously *in vitro*,^{2,12} but not in cells.

We next determined if we could use **1** to visualize ADP-ribosylated PARP10 in cells using fluorescence microscopy. In cells treated with **1** followed by click conjugation to rhodamine-azide after fixation we detected fluorescent labeling that colocalized with GFP-PARP10 WT (Figure 3b,c and Supporting Figure 3). The discrete localization of PARP10 protein and activity in large puncta in the cytoplasm is consistent with previous PARP10 localization studies.²¹ Importantly, we did not detect labeling in cells expressing GFP-PARP10 GW (Figure 3b,c and Supporting Figure 3). Together, these results demonstrate the utility of **1** for detecting PARP10 catalytic activity in cells.

While these results demonstrate that **1** can efficiently detect the activity of PARP10 in cells, we wanted to determine if **1** could be used to detect the activity of others PARPs that catalyze ADP-ribosylation on acidic amino acids on protein targets in cells. We first determined if we could detect the activity of PARP11, which catalyzes mono-ADP-ribosylation, presumably on acidic amino acids.² Consistent with a recent study, we found that GFP-PARP11 localized in a distinct punctate pattern in the nucleus.²² In cells treated with **1** followed by click conjugation to rhodamine-azide after fixation, we detected fluorescent labeling that colocalized with GFP-PARP11 (Supporting Figure 4). This result not only demonstrates that we can detect the activity in cells of another PARP that catalyzes mono-ADP-ribosylation but also confirms that PARP11 catalyzes ADP-ribosylation on acidic amino acids. We next focused on PARP1 and PARP2 since these PARPs are known to catalyze poly-ADP-ribosylation on acidic amino acids in protein targets. To stimulate PARP1/2 activity, we used hydrogen peroxide (H_2O_2), which activates PARP1/2 by inducing oxidative DNA damage in the nucleus.^{23,24} We observed extensive biotin labeling in HEK 293T cells treated with H_2O_2 (500 μ M) followed by treatment with **1** and PDA and subsequent click conjugation with biotin-azide in cell lysates (Figure 4a). This labeling was blocked by veliparib (3 μ M),²⁵ a potent inhibitor of PARP1/2, demonstrating that labeling by **1** is dependent on PARP1/2 activity (Figure 4a). Using rhodamine-azide during the click conjugation step on fixed cells demonstrated that the H_2O_2 -induced labeling was confined to the nucleus (Figure 4b), which is consistent with previous studies using an antibody specific for poly-ADP-ribosylation.^{24,26} The nuclear specific labeling was also blocked by veliparib

(Figure 4b). Together, these results demonstrate that **1** can be used to detect stimulus-induced, endogenous ADP-ribosylation.

In summary, AO-alkyne not only provided new insights into the mechanism of ADP-ribosylation on acidic amino acids but also demonstrated utility as a probe to detect both mono- and poly-ADP-ribosylation in cells. Given that acidic amino acids are major targets of ADP-ribosylation in cells, AO-alkyne will be a useful probe for examining this modification in cells under various stimulation paradigms, and for detecting changes in ADP-ribosylation in diseased cells (e.g., cancer cells). Moreover, AO-alkyne can be used to examine ADP-ribosylation of acidic amino acids on a subcellular level, which will provide important insight into the spatial regulation of ADP-ribosylation in cells.

METHODS

Chemical Synthesis

General—¹H NMR spectra were recorded on a Bruker DPX spectrometer at 400 MHz. Chemical shifts are reported as parts per million (ppm) downfield from an internal tetramethylsilane standard or solvent references. Dichloromethane (DCM), pyridine (pyr), and *N,N*-diisopropylethylamine (DIPEA) were dried using a solvent purification system manufactured by Glass Contour, Inc. (Laguna Beach, CA). All other solvents were of ACS chemical grade (Fisher Scientific) and used without further purification unless otherwise indicated. Commercially available starting reagents were used without further purification. (Boc-aminoxy)acetic acid (98%, Acros Organics), trifluoroacetic acid pentafluorophenyl ester (TFA-OPfp, 98%, Sigma-Aldrich), and monopropargylamine (99%, Acros Organics) were used as received.

Pentafluorophenyl (Boc-aminoxy)acetate 3—(Boc-aminoxy)-acetic acid (100 mg, 0.523 mmol) and anhydrous pyridine (46 μ L, 0.570 mmol, 1.1 equiv) were dissolved in anhydrous DCM (3 mL). To the solution was added TFA-OPfp (176 mg, 0.628 mmol, 1.2 equiv), and the reaction was stirred at room temperature for 1 h. The reaction was concentrated *in vacuo*. The crude residue was redissolved in EtOAc (5 mL), washed with 5% aq. NaHCO₃ (3 \times 5 mL) and brine (1 \times 5 mL), dried over Na₂SO₄, filtered, and concentrated *in vacuo* to yield a white solid (133 mg, 71%) that was used in subsequent reactions without further purification. ¹H NMR (400 MHz, DMSO-*d*₆): δ 10.41 (s, 1H), 4.89 (s, 2H), 1.42 (s, 9H).

2-(Boc-aminoxy)-N-propargylacetamide 4—Compound **3** (80 mg, 0.224 mmol) was dissolved in anhydrous DCM (3 mL), followed by the addition of DIPEA (43 μ L, 0.246 mmol, 1.1 equiv) and propargylamine (16 μ L, 0.250 mmol, 1.1 equiv). The reaction was stirred at room temperature for 1 h, after which the DCM was removed *in vacuo*. The crude residue was redissolved in EtOAc (5 mL), washed with 5% aq. NaHCO₃ (3 \times 5 mL) and brine (1 \times 5 mL), dried over Na₂SO₄, filtered, and concentrated *in vacuo* to yield a light yellow oil (49 mg, 96%) that was used in the following deprotection step without further protection. ¹H NMR (400 MHz, DMSO-*d*₆): δ 10.28 (s, 1H), 8.39 (t, 1H), 4.18 (s, 2H), 3.91 (dd, 2H), 3.13 (t, 1H), 1.41 (s, 9H).

2-Aminoxy-N-(propargyl)acetamide (AO-alkyne) 1—Compound **4** (22 mg, 0.096 mmol) was dissolved in 4 N HCl in dioxane (1.9 mL), and the reaction was stirred at room temperature for 1 h, in which a yellow color gradually developed. The reaction was concentrated *in vacuo*. The crude yellow residue was taken up in a minimal amount of MeOH (1 mL) and precipitated into anhydrous Et₂O (20 mL) to form a cloudy suspension. After storage at –20 °C overnight, a precipitate formed, which was collected via centrifugation. The solid was rinsed with Et₂O (10 mL) and dried *in vacuo* to yield the HCl salt of the product as a light orange solid (10 mg, 63%). ¹H NMR (400 MHz, DMSO-*d*₆): δ 10.74 (bs, 3H), 8.70 (t, 1H), 4.49 (s, 2H), 3.91 (dd, 2H), 3.18 (t, 1H).

Other Methods

Cloning and Mutagenesis—cDNA encoding human PARP10 was obtained from a HeLa cell cDNA library. cDNA encoding mouse PARP11 was obtained from a mouse embryonic day 16 cDNA library. Full-length PARP11 was cloned into pEGFP-C1 (Clontech). The catalytic domain (residues 809–1017) of PARP10 was PCR-amplified from the cDNA library using primers with noncomplementary restriction enzyme sites located at the 5′ and 3′ ends. The catalytic domain (residues 481–661) of PARP15 was PCR-amplified from a synthetic PARP15 (human) gene fragment (GeneArt Strings DNA Fragments, Life Technologies) using primers with noncomplementary restriction enzyme sites located at the 5′ and 3′ ends. Amplified products for both PARP10_{cat} and PARP15_{cat} were cloned into pET-28b+ (Novagen) for expression. The construct for His-tagged SRPK2 (human) was obtained from Addgene (Plasmid #39047) in pNIC28-Bsa4 and contains a deletion of internal segment 268–518. The construct for full length GFP-tagged PARP10 for mammalian expression was obtained from Paul Chang at Massachusetts Institute of Technology (Cambridge, MA). The PARP10 G888W (GW) mutant was generated using the QuickChange II XL site-directed mutagenesis kit (Agilent). Plasmids were sequenced from both the 5′ and 3′ direction to confirm the coding sequence.

Expression and Purification of PARP10_{cat}, PARP15_{cat}, and SRPK2—PARP10_{cat}, PARP15_{cat}, and SRPK2 were expressed in the *Escherichia coli* BL21 pRARE2 strain (EMD Millipore). Cells were first cultured in LB medium overnight at 225 rpm and 37 °C in an Excella E24 Incubator (New Brunswick Scientific). One liter of TB medium (12 g Bacto Tryptone (BD Biosciences), 24 g of Bacto Yeast Extract (BD Biosciences), 0.4% glycerol, 17 mM KH₂PO₄, 72 mM KHPO₄, 50 μg/mL kanamycin, and 34 μg/mL chloramphenicol) were inoculated with the starting culture and grown to OD₆₀₀ = 0.8–1.0 at 225 rpm and 37 °C. The temperature was reduced to 16 °C, and expression was induced by adding isopropyl β-d-thiogalactoside (IPTG) to 0.4 mM. After incubation at 16 °C for 18–24 h, cells were harvested by centrifugation at 6000g for 10 min. The cell pellet was resuspended in a lysis buffer (100 mM HEPES, pH 7.5, 0.5 mM tris(2-carboxyethyl)-phosphine hydrochloride (TCEP-HCl, Thermo Scientific Pierce), 500 mM NaCl, 10 mM imidazole, 10% glycerol, 1 mM benzamidine, 1 mM phenylmethylsulfonyl fluoride (PMSF), 8.3 mg/L DNase I (Roche)) at 4 °C, subjected to cell lysis using a Sonifier 450 (Branson) at 4 °C, and the resulting lysate was clarified by centrifugation at 12 000g for 30 min at 4 °C. Lysates were incubated with prewashed Ni-NTA agarose resin (50% slurry, Qiagen) with end-over-end rotation at 4 °C for 1 h. Following extensive washing with buffer B1 + 25 (20 mM HEPES,

pH 7.5, 0.5 mM TCEP-HCl, 1 mM PMSF, 1 mM benzamidine, 500 mM NaCl, 25 mM imidazole), protein was eluted in buffer B1 + 200 (20 mM HEPES, pH 7.5, 0.5 mM TCEP-HCl, 500 mM NaCl, 200 mM imidazole) for PARP10_{cat} and PARP15_{cat} and B1 + 100 (20 mM HEPES, pH 7.5, 0.5 mM TCEP-HCl, 500 mM NaCl, 100 mM imidazole) for SRPK2. Fractions containing desired protein were collected and dialyzed to 50 mM Tris-HCl, pH 7.5, 0.1 mM EDTA, 1 mM β -Me, and 0.4 M NaCl at 4 °C. Protein concentrations were determined by Bradford assay with BSA standards, and purity was assessed by PageBlue staining (Pierce) after SDS-polyacrylamide gel electrophoresis (SDS-PAGE). Greater than or equal to 90% purity was achieved for PARP10_{cat} and PARP15_{cat}. Greater than or equal to 50% purity was achieved for SRPK2.

ADP-ribosylation Assay for PARP10 with AO-alkyne Labeling and Immunoblot Detection—A total of 810 ng of PARP10_{cat} and 2.8 μ g of SPRK2 were incubated with 100 μ M NAD⁺ in a reaction buffer (50 mM Tris-HCl pH 8.0, 100 mM NaCl, 4 mM MgCl₂, 0.5 mM TCEP-HCl) at 30 °C for 1 h. The reaction was quenched by the addition of 10% SDS to a final concentration of 2%. A 3.5 \times stock of AO-alkyne at pH 5 (525 mM acetate, 787.5 mM NaCl), pH 6, pH 7, and pH 8 (all 525 mM phosphate, 787.5 mM NaCl) with or without catalyst (at 35 mM) was added to the reaction mixture (final [AO-alkyne] = 100 μ M) and incubated at room temperature for 1 h. A 4 \times stock of CB (400 μ M of tris[(1-benzyl-1H-1,2,3-triazol-4-yl)methyl]amine (TBTA), 4 mM CuSO₄, 400 μ M biotin-azide (Biotin-PEG3-Azide, Click Chemistry Tools), 4 mM TCEP-HCl in 1 \times phosphate buffered saline (PBS) with 1% SDS) was added to the reaction mixture (final [biotin-azide] = 100 μ M) and incubated at room temperature for 30 min. A 4 \times sample buffer with 5% β -mercaptoethanol (BME) was added. The reaction was diluted 1:40 with a 1 \times sample buffer prior to fractionation by SDS-PAGE, and subsequent immunoblot detection was performed using a ChemiDoc MP Imaging System (Bio-Rad). Coomassie staining was performed on undiluted reaction mixtures after fractionation by SDS-PAGE. Each experiment was repeated at least twice; shown are representative images.

ADP-ribosylation Assay for PARP10 and PARP15 with AO-alkyne Labeling and Fluorescence Detection—A total of 405 ng of either PARP10_{cat} or PARP15_{cat} and 1.4 μ g of SPRK2 were incubated with NAD⁺ (0, 1, 10, 50, 100 μ M) in reaction buffer (50 mM Tris-HCl pH 8.0, 100 mM NaCl, 4 mM MgCl₂, 0.5 mM TCEP-HCl) at 30 °C for 1 h. The reaction was quenched by the addition of 10% SDS to a final concentration of 2%. A 3.5 \times stock of AO-alkyne at pH 5 (525 mM acetate, 787.5 mM NaCl, 35 mM PDA) was added to the reaction mixture (final [AO-alkyne] = 100 μ M) and incubated at room temperature for 1 h. A 4.5 \times stock of CB (450 μ M of TBTA, 4.5 mM CuSO₄, 450 μ M rhodamine-azide (Sulforhodamine B Azide, Click Chemistry Tools), 4.5 mM TCEP-HCl in 1 \times PBS with 1% SDS) was added to the reaction mixture (final [rhodamine-azide] = 100 μ M) and incubated at room temperature for 30 min. A 4 \times sample buffer (with 5% BME) was added prior to fractionation by SDS-PAGE, and subsequent fluorescence detection was performed using a ChemiDoc MP Imaging System (Bio-Rad). Coomassie staining of the same gel was performed after fluorophore visualization.

Borohydride Reduction—ADP-ribosylation of SRPK2 by PARP10_{cat} was performed as outlined above except using 911 ng of PARP10_{cat} and 3.15 μ g of SRPK2 with either NAD⁺ or 6-a-NAD⁺ at 100 μ M. The reaction was quenched by the addition of 10% SDS to a final concentration of 2%. The reaction mixture was aliquoted, and 3 \times NaBH₄ solutions in 1 \times PBS were added for final concentrations of 10 mM NaBH₄, 1 mM NaBH₄, and PBS only (no NaBH₄). The reaction was incubated at room temperature for 15 min. A 4.5 \times stock of AO-biotin (Aldehyde Reactive Probe, ARP, Cayman Chemical) in pH 5 buffer (675 mM acetate, 1 M NaCl, 45 mM PDA) or a 4.5 \times stock of biotin-azide in pH 5 CB (675 mM acetate, 1 M NaCl, 450 μ M of TBTA, 4.5 mM CuSO₄, 450 μ M biotin-azide, 4.5 mM TCEP-HCl) was added for a final concentration of 100 μ M for both AO-biotin and biotin-azide. The reaction was incubated at room temperature for 1 h prior to dilution with a 4 \times sample buffer (with 5% BME). The reaction was diluted 1:20 with a 1 \times sample buffer prior to fractionation by SDS-PAGE, and subsequent immunoblot detection was performed using a ChemiDoc MP Imaging System. Coomassie staining was performed after fractionation by SDS-PAGE on undiluted reaction mixtures of a replicate experiment performed with twice the amount of both PARP10_{cat} and SRPK2. Each experiment was repeated at least twice; shown are representative images.

Dual Fluorophore Labeling—ADP-ribosylation of SRPK2 by PARP10_{cat} was performed as outlined above using 810 ng of PARP10_{cat} and 2.8 μ g of SRPK2 with 6-a-NAD⁺ at 100 μ M. The reaction was quenched by the addition of 10% SDS to a final concentration of 2%. A 3.5 \times stock of AO-TAMRA (Aminoxy-5(6)-TAMRA, Cayman Chemical) in pH 5 buffer (525 mM acetate, 787.5 mM NaCl, 35 mM PDA) or a 3.5 \times mock solution (containing all components except substitution of DMSO for AO-TAMRA) was added to the reaction mixture (final [AO-TAMRA] = 100 μ M). The reaction was incubated at room temperature for 1 h. A 4.5 \times stock of CB (450 μ M of TBTA, 4.5 mM CuSO₄, 450 μ M AF488-azide (Alexa Fluor 488 Azide, Life Technologies), 4.5 mM TCEP-HCl in 1 \times PBS with 1% SDS) or a 4.5 \times mock solution (containing all components except substitution of DMSO for AF488-azide) was added to the reaction mixture (final [AF488-azide] = 100 μ M) and incubated at room temperature for 30 min. A 4 \times sample buffer (with 5% BME) was added prior to fractionation by SDS-PAGE. Imaging was performed on a Typhoon 9400 (GE Healthcare Life Sciences) using recommended laser settings and filter sets for AF488 (Ex, 488 nm; PMT, 400 V; Em, 526 nm SP) and TAMRA (Ex, 532 nm; PMT, 400 V; Em, 580 nm BP 30 nm). Coomassie staining of the same gel was performed after fluorophore visualization. Each experiment was repeated at least twice; shown are representative images.

Cell Culture and Reagents—HEK 293T cells were grown at 37 °C and 5% CO₂. Cells were passaged in DMEM + 10% FBS (Gibco) + penicillin/streptomycin (Invitrogen). Antibodies used for immunoblot detection were α -GFP (ab13970, Abcam) and goat α -chicken IgY-HRP (sc-2428, Santa Cruz Biotechnology). Primary antibodies (stored at 1 mg mL⁻¹) were used at 1:5000 and secondary antibodies at 1:5000 for immunoblot assays. Streptavidin-HRP (Jackson ImmunoR-esearch) was stored at -20 °C in a 50% glycerol mix (0.5 mg mL⁻¹) and was used at 1:1000 for immunoblot assays.

Transfection of HEK 293T Cells—HEK 293T cells were grown in six-well plates to a confluency of 80–90%. Cells were transfected with 2 μg of plasmid DNA using standard CalPhos (Clontech) transfection techniques. After incubation for 7 h, cells were washed with medium (1 mL) and fed fresh medium (2 mL) and allowed to grow overnight. Transfection efficiency was verified via microscopy and ranged from 50 to 60%.

H₂O₂ Treatment of HEK 293T Cells—HEK 293T cells were grown in six-well plates to a confluency of 50–60%. Cells were pretreated with medium containing veliparib (3 μM) or DMSO for 10 min. Half of the medium was removed, and 2 \times H₂O₂ was added. This medium was added back to cells (final [H₂O₂] = 500 μM) and incubated for 15 min.

AO-Alkyne Cellular Labeling and Click Conjugation of Lysates—Cells were treated with **1** (100 μM) and PDA (10 mM) and incubated for 1 h. The medium was removed and cells were washed with cold (4 °C) PBS and lysed by freezing in N₂ (l) and thawing in either cold PBS or buffer containing 25 mM HEPES at pH 7.5, 50 mM NaCl, 10% glycerol, 1% Nonidet P-40 (NP-40), and 1 \times complete EDTA-free protease inhibitor cocktail (Roche) and subjected to centrifugation at 5000g for 5 min for PBS samples at 4 °C and 14 000g for 5 min at 4 °C for all other samples. Total protein concentration in the lysate was determined by Bradford assay with a BSA standard curve. Lysates containing normalized protein levels were subjected to click conjugation with 9 \times CB (900 μM of TBTA, 9 mM CuSO₄, 900 μM biotin-azide, 9 mM TCEP-HCl in 1 \times PBS with 1% SDS) and incubated at room temperature for 30 min. A 4 \times sample buffer (with 5% BME) was added prior to fractionation by SDS-PAGE.

Click Conjugation of AO-alkyne Labeled Cells and Microscopy—Cells were labeled with **1** as above. The medium was removed and replaced with fresh medium for 5 min. Cells were washed with 1 \times PBS and fixed with 4% PFA in 1 \times PBS for 15 min at room temperature. The cells were washed 3 \times 5 min with 1 \times PBS. Cells were permeabilized with 0.2% Triton X-100 in 1 \times PBS for 5 min at room temperature followed by washing with 1 \times PBS for 5 min. The cells were blocked in 3% BSA in 1 \times PBS at 4 °C for 2 h. The Click-iT Cell Reaction Buffer Kit (Life Technologies) was used for in-cell click conjugation of rhodamine-azide (1 μM , Sulforhodamine B Azide, Click Chemistry Tools). Cells were washed 2 \times with 3% BSA and ddH₂O. Coverslips were mounted with ProLong Gold Antifade Mountant with DAPI (Life Technologies). Images were taken on a Zeiss ApoTome wide-field microscope with the following channel parameters: blue, Ex: 380/40, Em: 445/50; green, Ex: 470/40, Em: 525/50; red: Ex: 545/ 25, Em: 605/70 and objectives: 20 \times 0.8 PlanApo, 60 \times 1.4 PlanApo. Images were processed in Zen 2012 (Zeiss) and levels were linearly adjusted in Adobe Photoshop CS5.

Supplemental Material

Refer to Web version on PubMed Central for supplementary material.

Acknowledgments

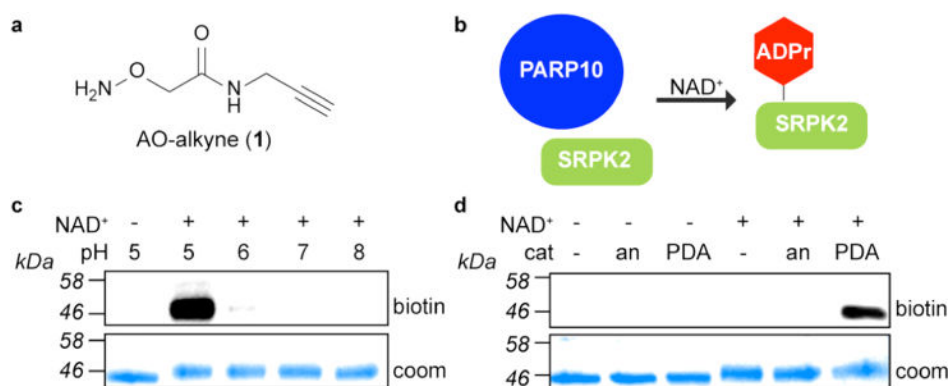
We thank P. Chang (MIT) for providing GFP-PARP10, T. Scanlan (OHSU) and I. Carter-O'Connell (OHSU) for advice on the manuscript, and members of the Cohen laboratory for many helpful discussions. This work was

supported by an Achievement Rewards for College Scientists (ARCS) Scholarship and National Institutes of General Medicine Training Grant T32GM071338 (R.K.M) and National Institutes of Neurological Disorders and Stroke NS088629 (M.S.C.).

References

1. Gibson BA, Kraus WL. New insights into the molecular and cellular functions of poly(ADP-ribose) and PARPs. *Nat Rev Mol Cell Biol.* 2012; 13:411–424. [PubMed: 22713970]
2. Vyas S, Matic I, Uchima L, Rood J, Zaja R, Hay RT, Ahel I, Chang P. Family-wide analysis of poly(ADP-ribose) polymerase activity. *Nat Commun.* 2014; 5:4426. [PubMed: 25043379]
3. Zhang J. Use of biotinylated NAD to label and purify ADP-ribosylated proteins. *Methods Enzymol.* 1997; 280:255–265. [PubMed: 9211321]
4. Jiang H, Kim JH, Frizzell KM, Kraus WL, Lin H. Clickable NAD Analogues for Labeling Substrate Proteins of Poly(ADP-ribose) Polymerases. *J Am Chem Soc.* 2010; 132:9363–9372. [PubMed: 20560583]
5. Carter-O'Connell I, Jin H, Morgan RK, David LL, Cohen MS. Engineering the Substrate Specificity of ADP-Ribosyltransferases for Identifying Direct Protein Targets. *J Am Chem Soc.* 2014; 136:5201–5204. [PubMed: 24641686]
6. Daniels CM, Ong S, Leung AKL. Phosphoproteomic Approach to Characterize Protein Mono- and Poly(ADP-ribosylation) Sites from Cells. *J Proteome Res.* 2014; 13:3510–3522. [PubMed: 24920161]
7. Zhang Y, Wang J, Ding M, Yu Y. Site-specific characterization of the Asp- and Glu-ADP-ribosylated proteome. *Nat Methods.* 2013; 10:981–984. [PubMed: 23955771]
8. Riquelme PT, Burzio LO, Koide SS. ADP ribosylation of rat liver lysine-rich histone *in vitro*. *J Biol Chem.* 1979; 254:3018–3028. [PubMed: 218960]
9. Bredehorst R, Wielckens K, Garemann A, Lengyel H, Klapproth K, Hilz H. Two Different Types of Bonds Linking Single ADP-Ribose Residues Covalently to Proteins. *Eur J Biochem.* 1978; 92:129–135. [PubMed: 729585]
10. Feijs KL, Kleine H, Braczynski A, Forst AH, Herzog N, Verheugd P, Linzen U, Kremmer E, Luscher B. ARTD10 substrate identification on protein microarrays: regulation of GSK3 β by mono-ADP-ribosylation. *Cell Commun Signal.* 2013; 11:5. [PubMed: 23332125]
11. Venkannagari H, Fallarero A, Lüscher B, Lehtiö L. Activity-based assay for human mono-ADP-ribosyltransferases ARTD7/PARP15 and ARTD10/PARP10 aimed at screening and profiling inhibitors. *Eur J Pharm Sci.* 2013; 49:148–156. [PubMed: 23485441]
12. Kleine H, Poreba E, Lesniewicz K, Hassa PO, Hottiger MO, Litchfield DW, Shilton BH, Luscher B. Substrate-assisted catalysis by PARP10 limits its activity to mono-ADP-ribosylation. *Mol Cell.* 2008; 32:57–69. [PubMed: 18851833]
13. Wendeler M, Grinberg L, Wang X, Dawson PE, Baca M. Enhanced Catalysis of Oxime-Based Bioconjugations by Substituted Anilines. *Bioconjugate Chem.* 2014; 25:93–101.
14. Moyle PM, Muir TW. Method for the Synthesis of Mono-ADP-ribose Conjugated Peptides. *J Am Chem Soc.* 2010; 132:15878–15880. [PubMed: 20968292]
15. Chaikin SW, Brown WG. Reduction of Aldehydes, Ketones and Acid Chlorides by Sodium Borohydride. *J Am Chem Soc.* 1949; 71:122–125.
16. Jankevicius G, Hassler M, Golia B, Rybin V, Zacharias M, Timinszky G, Ladurner AG. A family of macrodomain proteins reverses cellular mono-ADP-ribosylation. *Nat Struct Mol Biol.* 2013; 20:508–514. [PubMed: 23474712]
17. Rosenthal F, Feijs KLH, Frugier E, Bonalli M, Forst AH, Imhof R, Winkler HC, Fischer D, Caflisch A, Hassa PO, Luscher B, Hottiger MO. Macrodomain-containing proteins are new mono-ADP-ribosylhydrolases. *Nat Struct Mol Biol.* 2013; 20:502–507. [PubMed: 23474714]
18. Chen D, Vollmar M, Rossi MN, Phillips C, Kraehenbuehl R, Slade D, Mehrotra PV, von Delft F, Crosthwaite SK, Gileadi O, Denu JM, Ahel I. Identification of Macrodomain Proteins as Novel O-Acetyl-ADP-ribose Deacetylases. *J Biol Chem.* 2011; 286:13261–13271. [PubMed: 21257746]

19. Peterson FC, Chen D, Lytle BL, Rossi MN, Ahel I, Denu JM, Volkman BF. Orphan macrodomain protein (human C6orf130) is an O-acyl-ADP-ribose deacylase: solution structure and catalytic properties. *J Biol Chem.* 2011; 286:35955–35965. [PubMed: 21849506]
20. Yu M, Schreek S, Cerni C, Schamberger C, Lesniewicz K, Poreba E, Vervoorts J, Walsemann G, Grotzinger J, Kremmer E, Mehraein Y, Mertsching J, Kraft R, Austen M, Luscher-Firzloff J, Luscher B. PARP-10, a novel Myc-interacting protein with poly(ADP-ribose) polymerase activity, inhibits transformation. *Oncogene.* 2005; 24:1982–1993. [PubMed: 15674325]
21. Kleine H, Herrmann A, Lamark T, Forst AH, Verheugd P, Luscher-Firzloff J, Lippok B, Feijs KLH, Herzog N, Kremmer E, Johansen T, Muller-Newen G, Luscher B. Dynamic subcellular localization of the mono-ADP-ribosyltransferase ARTD10 and interaction with the ubiquitin receptor p62. *Cell Commun Signal.* 2012; 10:28. [PubMed: 22992334]
22. Meyer-Ficca ML, Ihara M, Bader JJ, Leu NA, Beneke S, Meyer RG. Spermatid Head Elongation with Normal Nuclear Shaping Requires ADP-Ribosyltransferase PARP11 (ARTD11) in Mice. *Biol Reprod.* 2015; 92:1.
23. Schraufstatter IU, Hinshaw DB, Hyslop PA, Spragg RG, Cochrane CG. Oxidant injury of cells. DNA strand-breaks activate polyadenosine diphosphate-ribose polymerase and lead to depletion of nicotinamide adenine dinucleotide. *J Clin Invest.* 1986; 77:1312–1320. [PubMed: 2937805]
24. Amé JC, Rolli V, Schreiber V, Niedergang C, Apiou F, Decker P, Muller S, Hoger T, Menissier-de Murcia J, de Murcia G. PARP-2, A novel mammalian DNA damage-dependent poly(ADP-ribose) polymerase. *J Biol Chem.* 1999; 274:17860–17868. [PubMed: 10364231]
25. Donawho CK, Luo Y, Luo Y, Penning TD, Bauch JL, Bouska JJ, Bontcheva-Diaz VD, Cox BF, DeWeese TL, Dillehay LE, Ferguson DC, Ghoreishi-Haack NS, Grimm DR, Guan R, Han EK, Holley-Shanks RR, Hristov B, Idler KB, Jarvis K, Johnson EF, Kleinberg LR, Klinghofer V, Lasko LM, Liu X, Marsh KC, McGonigal TP, Meulbroek JA, Olson AM, Palma JP, Rodriguez LE, Shi Y, Stavropoulos JA, Tsurutani AC, Zhu GD, Rosenberg SH, Giranda VL, Frost DJ. ABT-888, an Orally Active Poly(ADP-Ribose) Polymerase Inhibitor that Potentiates DNA-Damaging Agents in Preclinical Tumor Models. *Clin Cancer Res.* 2007; 13:2728–2737. [PubMed: 17473206]
26. Bürkle A, Chen G, Küpper JH, Grube K, Zeller WJ. Increased poly(ADP-ribosylation) in intact cells by cisplatin treatment. *Carcinogenesis.* 1993; 14:559–561. [PubMed: 8472314]

**Figure 1.**

AO-alkyne, a clickable aminoxy probe that can detect ADP-ribosylation of acidic amino acids. (a) Structure of bifunctional probe, AO-alkyne (1). The probe contains an aminoxy group for conjugation with the ADPr modification on acidic amino acids and an alkyne handle for subsequent click conjugation with an azido reporter. (b) Schematic showing PARP10 transferring the ADPr moiety of NAD⁺ onto its protein target SRPK2. (c) AO-alkyne-mediated labeling of ADPr-modified SRPK2 is pH dependent. SRPK2 was ADP-ribosylated by human PARP10 catalytic domain (hPARP10_{cat}) in the presence of NAD⁺ (100 μM). AO-alkyne selectively labels ADPr-modified SRPK2 in pH 5 acetate buffer as demonstrated by click conjugation with biotin-azide (100 μM). Proteins were resolved by SDS/PAGE and detected by Western blot with Streptavidin-HRP. (d) *p*-phenylenediamine (PDA, 10 mM) catalyzes the labeling of ADPr-modified SRPK2 by 1. ADPr-modified SRPK2 in pH 7 phosphate buffer was treated with 1 (100 μM) followed by click conjugation with biotin-azide (100 μM). Proteins were resolved by SDS/PAGE and detected by Western blot with Streptavidin-HRP. In contrast to PDA, aniline (an) results in no labeling at pH 7. Coomassie (Coom) Brilliant Blue staining was used to demonstrate even loading.

**Figure 2.**

AO-alkyne reveals an unanticipated mechanism of ADP-ribosylation on acidic residues. (a) Proposed mechanism of PARP catalyzed ADP-ribosylation of acidic residues, glutamate (Glu) and aspartate (Asp). In this mechanism, the Glu/Asp side chain undergoes a 1'-2' transfer. The ribose ring is in equilibrium between its open and closed conformation. At acidic pH or in the presence of catalysis at neutral pH, **1** reacts with the free aldehyde at the C1' position, resulting in the formation of a stable oxime. (b) Borohydride reduction after ADP-ribosylation blocks labeling of SRPK2 by AO-biotin. SRPK2 was ADP-ribosylated by hPARP10_{cat} in the presence of NAD⁺ (100 μM). ADPr-modified SRPK2 was then treated with NaBH₄ for 15 min at RT prior to AO-biotin (100 μM) treatment at pH 5 with PDA catalysis. Click conjugation was then performed with biotin-azide (100 μM). Proteins were resolved by SDS/PAGE and detected by Western blot with Streptavidin-HRP. (c) Borohydride reduction does not result in a loss of the ADPr modification. SRPK2 was ADP-ribosylated by hPARP10_{cat} in the presence of the clickable NAD⁺ analogue, 6-a-NAD⁺ (100 μM). 6-a-ADPr-modified SRPK2 was then treated with NaBH₄ for 15 min at RT prior to AO-biotin (100 μM) treatment at pH 5 with PDA catalysis. Under some conditions, click conjugation was performed with biotin-azide (100 μM). Proteins were resolved by SDS/PAGE and detected by Western blot with Streptavidin-HRP. (d) Dual labeling of ADPr at the C1' position and at the N6 position of ADPr. SRPK2 was ADP-ribosylated by hPARP10_{cat} in the presence of 6-a-NAD⁺ (100 μM). AO-TAMRA (100 μM) was reacted with 6-a-ADPr-SRPK2 at pH 5 with the PDA catalysis followed by click conjugation of AF488-azide (100 μM). Proteins were resolved by SDS/PAGE and detected by in-gel fluorescence scanning (Typhoon 9400).

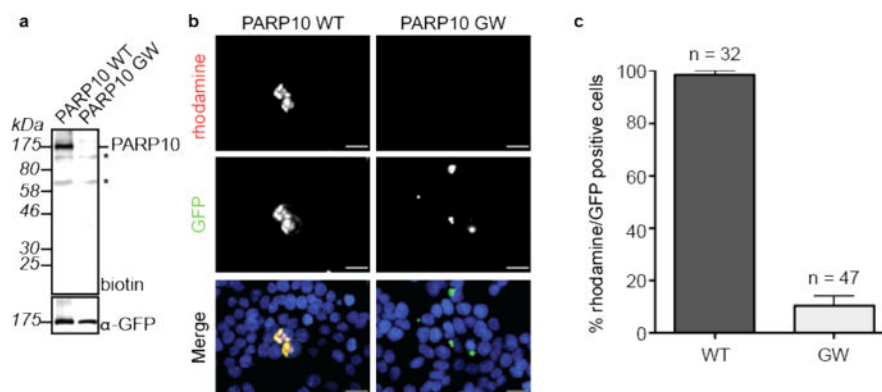


Figure 3.

AO-alkyne detects auto-ADP-ribosylation of PARP10 in cells. (a) HEK 293T cells expressing either GFP-PARP10 WT or GFP-PARP10 GW (catalytically dead) were treated with **1** (100 μ M) and PDA (10 mM) for 1 h at 37 $^{\circ}$ C. Lysates were then subjected to click conjugation with biotin-azide (100 μ M). Proteins were resolved by SDS/PAGE and detected by Western blot with either Streptavidin-HRP or an antibody against GFP. Bands marked with an asterisk represent endogenous biotinylated proteins. (b) HEK 293T cells overexpressing either GFP-PARP10 WT and GFP-PARP10 GW (catalytically dead) were treated similarly as in a. After fixation, permeabilization, and blocking, the cells were subjected to click conjugation with rhodamine-azide (1 μ M) for 30 min. Scale bar corresponds to 20 μ m. (c) Quantitation of rhodamine-positive HEK293T cells expressing GFP-PARP10 WT or GFP-PARP10 GW (see also Supporting Figure 3). The number of rhodamine-positive cells was normalized to GFP-positive cells for both GFP-PARP10 WT ($n = 32$) and GFP-PARP10 GW ($n = 47$). Error bars represent SEM.

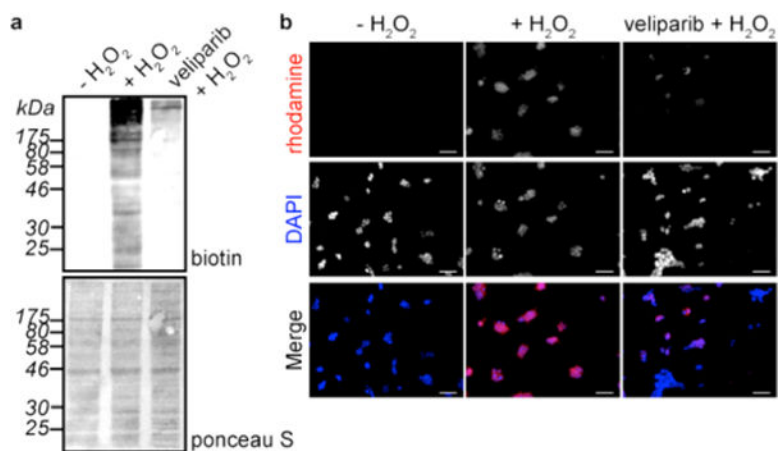


Figure 4.

AO-alkyne detects ADPr modification catalyzed by endogenous PARPs activated during oxidative stress. (a) HEK 293T cells were treated with H₂O₂ (500 μ M) for 15 min at 37 °C in the presence of the PARP1/2 inhibitor veliparib (3 μ M) or DMSO (control) followed by incubation with 1 (100 μ M) and PDA (10 mM) for 1 h at 37 °C. Lysates were subjected to click conjugation with biotin-azide (100 μ M) and analyzed via immunoblot. Staining of the membrane with Ponceau S serves as a loading control. (b) Cells were treated similarly as in a. After fixation, permeabilization, and blocking, the cells were subjected to click conjugation with rhodamine-azide (1 μ M) for 30 min. Scale bar corresponds to 50 μ m.